Design and Analysis of a Novel Transverse-Flux Tubular Linear Machine With Gear-Shaped Teeth Structure

J. F. Pan[1], Norbert C. Cheung[2], and Yu Zou[1]

[1]Department of Automation Science, College of Mechatronics and Control Engineering, Shenzhen University, Shenzhen 518060, China

[2]Department of Electrical Engineering, The Hong Kong Polytechnic University, Hunghom, Kowloon, Hong Kong, China

A transverse-flux tubular linear machine with novel gear-shaped teeth for high force density is proposed. The teeth can be formed by silicon steel laminations or permanent magnets for a tubular linear switched reluctance or tubular linear hybrid motor. With the unique improved teeth structure and short magnetic circulation paths, larger propulsion force output can be obtained with reduced mover weight and volume. Simulation based on finite element method (FEM) verifies the validity of the proposed machine design. The proposed machines are compared with other transverse-flux linear machines. Results show that the proposed tubular motors exhibit better output performance with a higher force-to-volume ratio.

Index Terms—**FEM, transverse-flux, tubular linear machine.**

I. Introduction

In industry, translational high-speed motion is in vast demand for manufacturing facilities such as laser soldering and printed circuit board (PCB) machines, etc. Linear motors with large force density per volume and high efficiency are an ideal solution to their rotary motors counterparts which need to be coupled with rotary to linear mechanical transformers [1]. In recent years, there is a surge of interests in the development of longitudinal-flux switched reluctance (SR) and permanent magnet (PM) motors [2], [3]. While in a transverse-flux type of SR or hybrid motor, magnetic flux is perpendicular to the direction of movement, which ensures a separation from magnetic circuit to electric circuit and a tight machine structure can be realized [4]–[6]. Compared with regular transverse-flux machines, a transverse-flux tubular linear machine has the advantages of simple manufacture, assembly process and small air gaps with low flux leakage and shorter flux paths [7]. Therefore, a more compact size, higher force-to-volume ratio machine structure can be realized in a transverse-flux tubular linear SR motor (TFTLSRM) or transverse-flux tubular linear hybrid motor (TFTLHM).

The transverse-flux tubular linear motors based on SR and hybrid machine principle are proposed in [7], [8] and [6], [10], respectively. They both employ an integral solid mover from soft magnetic composite material and are only dedicated to low-speed applications that low eddy current losses can be neglected. The TFTLSRM with square mover and stator configuration is proposed in [7] and a detailed design procedure is investigated. Since the machine utilizes single-sided topology, attraction force between the mover and stator cannot be neutralized and a smaller and uniform air gap is hard to achieve. A TFTLSRM with a round mover shaft is researched in [8]. Though machine structure is simple and robust, the motor utilizes stator end teeth and mover shaft for magnetic path circulation. The flux path is long and a large force-to-volume ratio is difficult to be realized.

For full utilization of the magnetic paths, a novel transverse-flux tubular linear machine with gear-shaped teeth structure is proposed. The gear material can be either silicon steel (SiS) laminations for a TFTLSRM or permanent magnet to form a TFTLHM. After the design procedure of the SiS-gear TFTLSRM and PM-gear TFTLHM, characteristic investigations based on finite element method (FEM) validate the design procedure. Performance analysis and comparison between the proposed motors and the square shape TFTLSRM and the machine with a round mover shaft are also carried out.

II. Machine Structure

As shown in Fig. 1, since the axis of movement is secured to axial direction (X-axis) only, the gear-shaped teeth serve as part of shorter flux circulation to achieve a more compact and effective magnetic path. The machine has an active moving body and a passive stator. The material from the movers and stator for the magnetic paths are made of SiS materials with laminations except that the gear-shaped teeth on the movers can be either silicon ferrite laminations or permanent magnets. The mover slots that connect to adjacent phases on the shaft are made from non-ferrite materials such as aluminum alloy.

From the front view illustrated in Fig. 1(b), windings A1–B4 can be excited simultaneously or independently as required. For more propulsion force output, more stator modules can be added as necessary with corresponding phase(s) serially connected. Compared with other transverse-flux linear motors, the salient advantages of the machine structure can be summarized as,

1) Machine structure is simple with low production cost.
2) Manufacturing and assembly process of the stator, mover and gear-shaped teeth is simpler since both the ferrite and non-ferrite segments are made in a modular structure and can be assembled easily.
3) Air gaps can be kept as a reasonable level and normal forces between the mover and stator can be theoretically neutralized.

Manuscript received March 01, 2012; revised April 25, 2012; accepted May 25, 2012. Date of current version October 19, 2012. Corresponding author: N. C. Cheung (e-mail: norbert.cheung@polyu.edu.hk).

Color versions of one or more of the figures in this paper are available online at http://ieeexplore.ieee.org.

Digital Object Identifier 10.1109/TMAG.2012.2202377

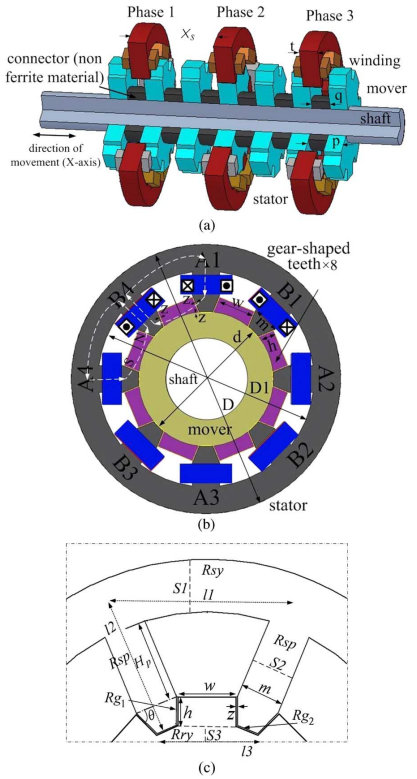

Fig. 1. The tubular linear machine (a) structure of one module (b) front view and (c) one section of the stator.

4) With the gear-shaped teeth, shorter and effective flux paths can be achieved and larger force-to-volume ratio can be expected.

From the machine structure, the introduction of the gear-shaped teeth facilitates a shorter magnetic circulation path as illustrated in Fig. 1(b), however, this arrangement inevitably sacrifices a more effective winding area compared with other TFTLSRMs proposed in [7] and [8]. The assembly of the linear guides is required to be precise for the machine since smaller air gaps should be maintained and the movement of the moving body should be mechanically locked in X-axis only.

III. Design Considerations

The TFTLSRM is designed for one axis of the laser soldering machine. The maximum linear velocity and acceleration time are specified as $V_m = 4.5$ m/s and $t_a = 0.3$ s, respectively. The acceleration is derived as

$$a = \frac{V_m}{t_a} = 15 \text{ m/s}^2. \tag{1}$$

Since the total weight of the movers with load does not exceed 10 kg, propulsion force for instantaneous acceleration is calculated as

$$F_m = M \cdot a = 150 \text{ N}. \tag{2}$$

The power capacity is derived as

$$P_m = F_m \cdot V_m = 675 \text{ W}. \tag{3}$$

Since the length of stator is restricted to 800 mm, to achieve a larger force output, six modules for each phase of the three phase are cascaded together with "18/24" SR machine topology. Then the number of poles for the stator and mover are $N_s = 18$ and $N_r = 24$. Stator pole pitch of $X_s = 40$ mm is selected and stator length L is calculated as

$$L = X_s \cdot N_s = 720 \text{ mm}. \tag{4}$$

Mover pole pitch is calculated as

$$p = \frac{L}{N_r} = 30 \text{ mm}. \tag{5}$$

Mover pole width is selected as 0.9–1.4 times of stator pole width t, q can be 15 mm if t is 14 mm for equally spaced stator pole width and slot.

The mechanical output power developed from the designed machine is [1]

$$P_m = U \cdot I \cdot k_d \cdot \eta. \tag{6}$$

where U and I are terminal voltage and current, respectively. η is efficiency and machine factor duty cycle K_d is determined by current conduction positions for each rising inductance profile, which is selected as 1.36. Since terminal voltage U can be represented as [7]

$$U = \frac{2 \cdot V_m}{t} \cdot B_g \cdot N \cdot S \cdot \left(1 - \frac{1}{\lambda}\right) \tag{7}$$

where B_g stands for flux density of air gap and N is the number of turns per stator pole. S is the total air gap area for each stator pole and it can be represented as

$$S = L_g \cdot t \tag{8}$$

λ is defined as the ratio between the inductance value from the fully aligned position L_a and the fully un-aligned position L_u.

Since the specific electric loading A_s (in A/m) is defined as [1]

$$A_s = \frac{3 \cdot N \cdot I}{N_r \cdot t}. \tag{9}$$

From (6)–(9), the total air gap length for each stator pole can be calculated as

$$L_g = \frac{P_m}{A_s \cdot B_g \cdot \eta \cdot V_m \cdot t \cdot K_d \cdot K} \tag{10}$$

with $K = ((2 \cdot N_r)/3) \cdot (1 - (1/\lambda))$.

With specific electric loading A_s, flux density B_g of air gap and maximum machine efficiency η assumed as 55000 A/m, 1.1 T and 70%, respectively, from the linear SR machine design principle, the total air gap length for each stator pole can be calculated as $L_g = 16.6$ mm.

As depicted in Fig. 2(c), if stator teeth width is set as $m = 9$ mm and $\theta = 67.5°$ for a parallel gear height, h can be derived by solving the equation as

$$2 \cdot h + (m - 2 \cdot h \cdot \cos\theta) = L_g \tag{11}$$

and we have $h = 6.16$ mm.

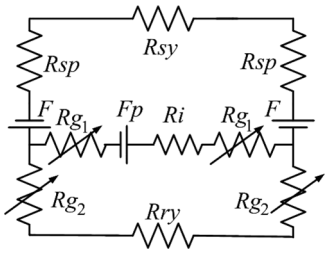

Fig. 2. Approximate magnetic path for one section.

The width of the three air gaps can be manufactured as small as typical rotary motors as $z = 0.3$ mm. Assuming maximum allowable current level in the winding as $I_m = 5$ A, the number of turns per each stator pole is

$$2 \cdot N = \frac{2 \cdot z \cdot B_g}{\mu_0 \cdot I_m} = 105. \tag{12}$$

Here N is selected as 60 turns. Assuming a current density limitation of $J = 6\ \mathrm{A/mm^2}$, the area of winding is calculated as [1]

$$S_a = \frac{I_m}{J \cdot \sqrt{\varphi}} = 0.481\ \mathrm{mm^2} \tag{13}$$

Then total winding area can be derived as

$$S_{Cu} = S_a \cdot N \approx 28.86\ \mathrm{mm^2}. \tag{14}$$

Supposing a fill factor of $K_s = 0.333$, area required for copper wire is calculated as

$$S = \frac{S_{Cu}}{K_s} = 86.67\ \mathrm{mm^2}. \tag{15}$$

To fully utilize winding area and obtain a uniform air gap width, the gear teeth width w is set as 8.56 mm. From Fig. 2(c), stator yoke height H_p can be obtained from the following equation as:

$$S = \left(\frac{w}{2} + H_p \cdot \cos\theta\right) \cdot H_p \cdot \sin\theta/2 \tag{16}$$

and we have $H_p = 17.2$ mm.

A yoke height of 18 mm is chosen for the stator. Assuming mover diameter (d) as 33 mm, inner stator yoke diameter D_1 can be derived as

$$D_1 = 2(\sin\theta \cdot h + H_p) + d = 80.4\ \mathrm{mm}. \tag{17}$$

Outer stator diameter D is calculated as

$$D = D_1 + 2 \cdot m = 98.4\ \mathrm{mm}. \tag{18}$$

The outer stator diameter of 100 mm is selected. Table I summarizes main specifications of the TFTLSRM.

If the SiS gear is replaced with PM, the equivalent magnetic path for one section can be approximated with the reluctance

TABLE I
TFTLSRM SPECIFICATIONS

Stator phase (φ)	3
Number of stator pole(N_s)	18
Number of mover pole(N_r)	24
Stator length(L)	720 mm
Travel distance	500 mm
Mover pole pitch/width (p/q)	30 /15 mm
Stator pole pitch/width (X_s/t)	40 /14 mm
Phase resistance	10 ohm
Number of turns per stator pole (N)	60
Gear height (h)	6.16 mm
Gear width (w)	8.56 mm
Mover diameter (d)	33 mm
Shaft diameter	25 mm
inner stator yoke diameter(D_1)	80.4 mm
Outer stator diameter(D)	100 mm
Air gap width (z)	0.3 mm

defined in Fig. 2 neglecting flux leakage. The magnetomotive forces from the windings and the PM are depicted as F and F_p, respectively. Under the linear region, the following equation can be derived when the PM gear is the only excitation source to provide flux-linkage Φ_p with inner reluctance of R_i,

$$F_p = (2 \cdot R_{g1} + 2 \cdot R_{sp} + R_{sy} + R_i) \cdot \Phi_p \tag{19}$$

If the only excitation source is the windings, then the equation for flux-linkage Φ can be represented as,

$$2 \cdot F = (2 \cdot R_{g2} + 2 \cdot R_{sp} + R_{sy} + R_{ry}) \cdot \Phi \tag{20}$$

For unsaturated region, total flux-linkage Φ_{total} can be assumed to be,

$$\Phi_{total} = \Phi_p + \Phi \tag{21}$$

Since the reluctance of the ferrite core is comparatively small at aligned positions, the ampere turns from the PM teeth can be approximately regarded as,

$$F_p = \sum_l H_c \cdot dl \approx H_c \cdot 2 \cdot z \tag{22}$$

where H_c is coercivity and l is total length of the magnetic path. If the PM material with a coercive force and remanence of 250000 A/m and 0.931 T from the bonded $NdFeB$ magnet are selected, F_p is about 150 A $\cdot$ m. It can be regarded as approximately an extra 50% magnetomotive force is excited to the TFTLHM at current excitation of 5 A, neglecting the saturation effect.

Assuming an average relative permeability of 9000 for the SiS, the sectional areas for stator yoke, teeth and effective mover magnetic path are $S1$, $S2$ and $S3$, respectively, as shown in

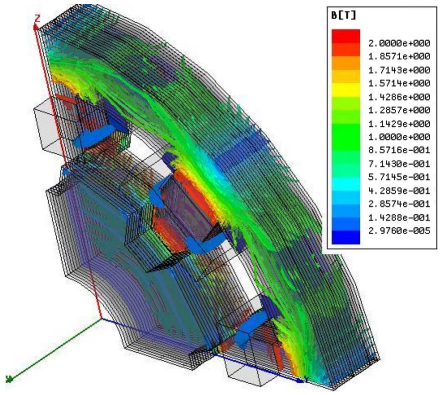

Fig. 3. Contour of flux density.

Fig. 1(c). The approximated ideal length for magnetic path circulation is represented as $l1$, $l2$ and $l3$. Then reluctance for Rsy, Rsp, Rry and Rg_2 can be calculated as,

$$Rsy = \frac{l1}{u_r u_0 S1} = 265.3, \quad Rsp = \frac{l2}{u_r u_0 S2} = 334.0$$
$$Rry = \frac{l3}{u_r u_0 S3} = 471.6 \quad \text{and} \quad Rg_2 = \frac{z}{u_0 S_g}$$
$$= 5.31 \times 10^4 \left(\frac{\text{A} \cdot \text{turns}}{\text{Wb}}\right)$$

where S_g is the sectional area for the air gap. Then inductance for one section of the machine as illustrated in Fig. 3(c) can be calculated as,

$$L_{\text{sec}} = \frac{(2 \cdot N)^2}{Rry + Rsy + 2 \cdot Rsp + 2 \cdot Rg_2} = 133.8 \text{ mH} \quad (23)$$

To verify the effectiveness of the approximate magnetic path approach, two-dimensional FEM calculation for one section is also been carried out with inductance result of 148.3 mH, which corresponds to the magnetic circuit derivation discussed above.

IV. Characteristics Analysis

A. Performance Prediction

The FEM-based analysis is applied to verify the design procedure for the TFTLSRM and TFTLHM. To fully inspect motor performance, three-dimensional (3D) model is built with stator and mover constructed in laminations stacked along X directions instead of a solid model to achieve a negligible eddy current effect. Fig. 2 demonstrates the flux distribution contour as the stator and mover teeth overlap with a current excitation level of 5 A. It can be seen that flux lines mainly distribute within the stator yoke, teeth and the gears to form a short magnetic circulation path. It can also been derived that the lamination structure ensures a flux distribution along the Y-Z plane only for each silicon ferrite plate.

The results of normal force calculation from Y and Z directions of any one complete stator for the TFTLSRM are illustrated in Fig. 4. Since normal force ripples fall below 0.35 N, it can be approximated that the normal forces between the mover and stator are negligible.

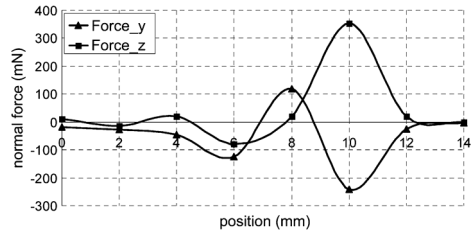

Fig. 4. Normal force calculations for the TFTLSRM.

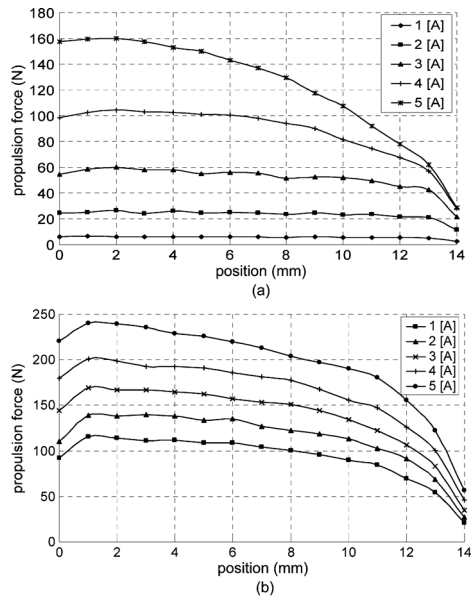

Fig. 5. Propulsion force of the (a) SiFe-gear and (b) PM-gear machine.

The propulsion force output profiles for the SiS-gear and PM-gear tubular linear machine can be found in Fig. 5 with current excitation from 1 to 5 A. The fully aligned position is 14.5 mm and the fully un-aligned position is 0 mm, measured from the mover to the stator. The force-to-volume ratio can be further boosted if SiS gears are replaced with PM gears. Maximum force reaches 159.5 N and 239.7 N for the TFTLSRM and TFTLHM, respectively. The force waveform descends faster for the TFTLSRM at fully un-aligned to fully aligned positions with current excitation above 4 A. Due to the introduction of PMs, the magnetic force from the PMs compensate for the sudden loss of current excitation at high levels and change of propulsion force is slow and gentle.

The calculation results of propulsion force v.s. different air gap lengths from 0.1 mm to 0.9 mm at rated current excitation level can be found in Fig. 6. It can be concluded that machine performance of the TFTLHM is sensitive to air gap lengths.

Machine efficiency can be derived from FEM as well. At current excitation of 5 A for one section, core loss and copper loss are calculated as 1.115 W and 5.934 W, respectively. Then machine efficiency for the TFTLSRM can be estimated as 64.8%.

B. Performance Comparison

The comparison on the performance of transverse-flux linear motors is based on the facts that the volume, total number of

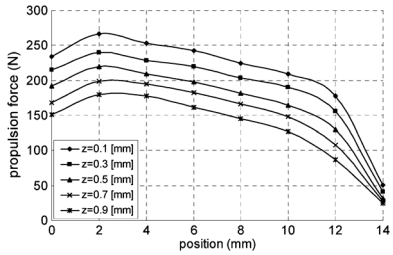

Fig. 6. Propulsion force of the PM-gear machine v.s. air gap.

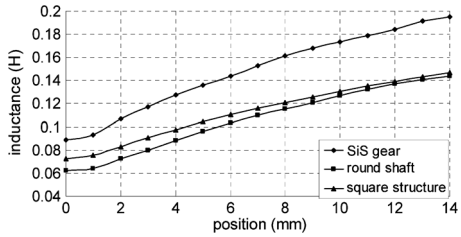

Fig. 7. Inductance profiles with no excitation.

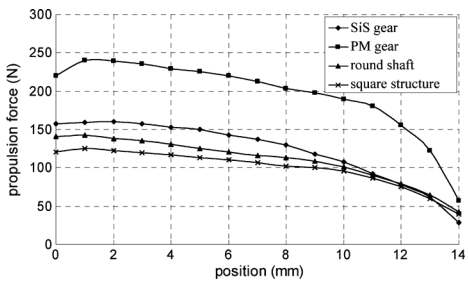

Fig. 8. Propulsion force comparison.

turns and SiS material applied are the same. Though the proposed TFTLSRM and the machines with either a square shape or a round mover shaft need further optimization process, for preliminary test, it can be expected that under the same condition, the proposed TFTLSRM exhibits a higher force-to-volume ratio owing to a shorter magnetic path structure.

Inductance is calculated using the 3D time-stepping FEM of the transient magnetic field mechanical motion coupled model with zero current excitation [11]. As shown in Fig. 7 the results of inductance profiles, inductance value for the TFTLSRM is larger when compared with tubular motors with a round shaft or square structure at different positions. Since the TFTLSRM possesses a more compact and shorter magnetic path, the change of inductance for the SiS-gear tubular machine is also bigger from fully un-aligned positions to fully aligned positions, and a higher force-to-volume ratio is expected.

Calculation of propulsion force outputs with current excitation of 5 A can be found in Fig. 8 for different tubular linear machines. It can be seen from the force waveforms that the TFTLHM with PM gears have larger propulsion force values. Among SR-based tubular linear machines, the TFTLSRM with SiS gears exhibits higher force-to-volume ratio which verifies the inductance calculations depicted in Fig. 7.

V. Conclusion

In this paper, a novel gear-shaped teeth structure is proposed for the design of TFTLSRM and TFTLHM with shorter magnetic paths and lower flux leakage. Both machines have a simple structure with low production cost. Compared with other transverse-flux tubular linear machines, the machines with either SiS gears or PM gears exhibit better output performance. Therefore, the gear-shaped teeth contribute to the optimization of tubular linear machine with higher force-to-volume ratio and efficiency.

Though normal force ripples from Y- or Z-axis can be treated negligible theoretically, the requirements for manufacture and assembly of the transverse-flux machines are high in order to ensure a uniform movement in X-axis only considering manufacturing and assembly tolerances. To maintain small and uniform air gaps between the stator teeth and the gear-shaped teeth, the authors consider that a square linear guide can be mounted in the mover shaft to facilitate the movement along X-axis and prevent the mover from rotation at the same time. The TFTLHM prototype is under construction and it can be expected that more experimental results such as the propulsion force and normal force ripples, etc. can be derived from the machine prototype.

Acknowledgment

This work was supported in part by the National Natural Science Foundation of China, Guangdong Natural Science Foundation and Hong Kong Research Grants Council under the code 51007059, S2011010001208 and PolyU5140/07E, and in part by the Shenzhen government fund JC201005280390A and ZYB200907080073A.

References

[1] R. Krishnan, *Switched Reluctance Motor Drives-Modeling, Simulation, Analysis, Design, and Applications*. Boca Raton, FL: CRC Press, 2001, pp. 18–22.

[2] Z. Zhang, N. C. Cheung, K. W. E. Cheng, X. D. Xue, and J. K. Lin, "Longitudinal and transversal end-effects analysis of linear switched reluctance motor," *IEEE Trans. Magn.*, vol. 47, no. 10, pp. 3979–3982, Oct. 2011.

[3] H. Lu, J. Zhu, Z. Lin, and Y. Guo, "A miniature short stroke linear actuator-design and analysis," *IEEE Trans. Magn.*, vol. 44, no. 4, pp. 497–504, Apr. 2008.

[4] B. L. J. Gysen, K. J. Meessen, J. J. H. Paulides, and E. A. Lomonova, "3-D analytical and numerical modeling of tubular actuators with skewed permanent magnets," *IEEE Trans. Magn.*, vol. 47, no. 9, pp. 2200–2212, Sep. 2011.

[5] G. Xiong and S. A. Nasar, "Analysis of fields and forces in a permanent magnet linear synchronous machine based on the concept of magnetic charge," *IEEE Trans. Magn.*, vol. 25, no. 3, pp. 2713–2719, May 1989.

[6] P. Zheng, C. Tong, G. Chen, R. Liu, Y. Sui, W. Shi, and S. Cheng, "Research on the magnetic characteristic of a novel transverse-flux PM linear machine used for free-piston energy converter," *IEEE Trans. Magn.*, vol. 47, no. 5, pp. 1082–1085, May 2011.

[7] B. Ge, A. T. de Almeida, and F. J. T. E. Ferreira, "Design of transverse flux linear switched reluctance motor," *IEEE Trans. Magn.*, vol. 45, no. 1, pp. 113–119, Jan. 2009.

[8] I.-A. Viorel, K. Hameyer, and L. Strete, "Transverse flux tubular switched reluctance motor," in *Proc. 11th Int. Conf. IEEE Optimization Electri. Electron. Equip.*, 2008, pp. 131–136.

[9] J.-F. Llibre, N. Martinez, B. Nogarède, and P. Leprince, "Linear tubular switched reluctance motor for heart assistance circulatory-analytical and finite element modeling," in *Proc.10th Int. Conf. IEEE Workshop ECMS.*, 2011, pp. 1–6.

[10] J. Wang, W. Wang, K. Atallah, and D. Howe, "Design considerations for tubular flux-switching permanent magnet machines," *IEEE Trans. Magn.*, vol. 44, no. 11, pp. 4026–4032, Nov. 2008.

[11] W. N. Fu and S. L. Ho, "Enhanced nonlinear algorithm for the transient analysis of magnetic field and electric circuit coupled problems," *IEEE Trans. Magn.*, vol. 45, no. 2, pp. 701–706, Feb. 2009.